Manipulating modern diesel engine particulate emission characteristics through butanol fuel blending and fuel injection strategies for efficient diesel oxidation catalysts

Fayad, MA, Tsolakis, A, Fernández-Rodríguez, D, Herreros, JM, Martos, FJ & Lapuerta, M

Original citation & hyperlink:
Fayad, MA, Tsolakis, A, Fernández-Rodríguez, D, Herreros, JM, Martos, FJ & Lapuerta, M 2017, 'Manipulating modern diesel engine particulate emission characteristics through butanol fuel blending and fuel injection strategies for efficient diesel oxidation catalysts' *Applied Energy*, vol 190, pp. 490-500
https://dx.doi.org/10.1016/j.apenergy.2016.12.102

DOI 10.1016/j.apenergy.2016.12.102
ISSN 0306-2619

Publisher: Elsevier

Manipulating modern diesel engine particulate emission characteristics through butanol fuel blending and fuel injection strategies for efficient diesel oxidation catalysts

M.A. Fayad[a,b], A. Tsolakis[a*], D. Fernández-Rodríguez[c], J.M. Herreros[a,d], F.J. Martos[e], and M. Lapuerta[c]

[a] School of Mechanical Engineering, University of Birmingham, Birmingham B15 2TT, UK

[b] Energy and Renewable Energies Technology Center, University of Technology, Baghdad, Iraq

[c] University of Castilla-La Mancha, Escuela Técnica Superior de Ingenieros Industriales, Edificio Politécnico. Avda. Camilo José Cela s/n, 13071 Ciudad Real, Spain

[d] Faculty of Engineering, Environment & Computing, Coventry University, Coventry. CV1 5FB, UK

[e] Escuela Técnica Superior de Ingeniería Industrial, University of Málaga, 29071, Málaga, Spain

* Corresponding author. Email: a.tsolakis@bham.ac.uk, tel.: +44 (0) 121 414 4170;

Abstract

Decoupling the dependences between emission reduction technologies and engine fuel economy in order to improve them both simultaneously has been proven a major challenge for the vehicle research communities. Additionally, the lower exhaust gas temperatures associated with the modern and future generation internal combustion engines are challenging the performance of road transport environmental catalysts. Studying how fuel properties and fuel injection strategies affect the combustion characteristics, emissions formation and hence catalysts performance can unveil synergies that can benefit vehicle emissions and fuel economy and as well as guide the design of next generation sustainable fuels. The experimental work presented here was conducted using a modern single-cylinder, common rail fuel injection system diesel engine equipped with a diesel oxidation catalyst (DOC). The impact of the fuel post-injection strategy that is commonly used as part of the aftertreatment system function (i.e. regeneration of diesel particulate filters or activity in hydrocarbon selective reduction of NO_X), combined with butanol-diesel fuel blend (B20) combustion on engine emissions formation, particulate matter characteristics (size distribution, morphology and structure) and oxidation catalyst activity were studied. It was found that post-injection produced lower PM concentration and modified the soot morphological parameters by reducing the number of primary particles (n_{po}), the radius of gyration (R_g), and the fractal dimension (D_f). The results were compared with the engine operation on diesel fuel. The increased concentration of HC and CO in the exhaust as a result of the diesel fuel post-injection at the studied exhaust conditions (i.e. T= 300 °C) led in the reduction of the DOC activity due to the increased competition of species for active sites. This effect was improved the combustion of B20 when compared to diesel.

Keywords: alternative fuels, diesel oxidation catalyst, gaseous emissions, particulate matter, post-injection, butanol

1. Introduction

With the view to improve the air quality, new engine and vehicle systems and technologies are under development in order to reduce pollutants emitted to the atmosphere especially in the very challenging transportation sector [1, 2]. In road transport, replacing fossil fuels with biofuels also provide cleaner combustion and consequently improve the efficiency of the catalytic aftertreatment systems and can be considered as a way to help vehicle manufacturers to achieve the emissions legislative limits such as the EURO 6 and CARB (LEV III) [3].

Bioalcohols and other oxygenated fuels have been reported to reduce emissions, when replacing gasoline fuels in spark-ignition (SI) engines. More recently these fuels have been studied as substitute to diesel fuel [4-8] because of their oxygen content that contributes in the reduction of the engine out CO, UHC (unburned hydrocarbons), NO_X (nitrogen oxides) and total PM emissions. It is reported that the hydroxyl group present in alcohols is more efficient in reducing diesel engine PM than other functional groups with the same oxygen content, especially at high engine loads [9-11]. The combustion of diesel-ethanol blends for example has been widely reported to reduce PM emissions [4, 12]. However, there are also drawbacks [13, 14] such as the ethanol's limited solubility in diesel fuel [15], the very low cetane number and the lower dynamic viscosity, parameters that can impact on the engine's operation and combustion characteristics [4, 16, 17]. Butanol in diesel has shown more promising characteristics as an alternative fuel to ethanol [4] due to higher cetane number and better solubility in diesel fuel as a consequence of being less polar that other alcohols with shorter chain. Furthermore, it has higher heating value, lower volatility, and less hydrophilic character [18, 19].

Modern engine after-treatment systems consist of different components such as the diesel oxidation catalysts (DOC) and diesel particulate filters (DPF) [20]. DOCs have a honeycomb monolith shape with high cell density (large surface area) and suitable loadings of a catalytic material such as platinum and/or palladium that is able to almost eliminate CO, HC and much of the particulate organic fraction [16, 20, 21]. DOC also oxidise NO to produce NO_2 that can then be utilised in the DPF to passively oxidise soot at low temperatures [16, 22, 23]. The DOC's activity depends on exhaust gas temperature, residence time of the exhaust gas in the catalyst, level and nature of gaseous and particulate matter exhaust species and inhibitions/synergies between the different species contained in the exhaust gas [23, 24]. In the same way, DPF performance is also influenced by size and morphology [fractal dimension (D_f), radius of gyration (R_g) and number of primary particles (n_{po})] of soot particles making understand their control challenging [16, 25]. Therefore, the effect of fuel and engine operating parameters such as injection settings (e.g. number of injections, injection timing, injection pressure, injection quantity) needs to be understood in order to improve not only the engine performance (power/torque) characteristics but also the function of the aftertreatment system [26]. Several studies

have shown that the post-injection in combination with the DOC is commonly used to increase the exhaust gas temperature in order to aid the DPF regeneration (i.e. active regeneration) [27].

The impact of fuel post-injection on engine out gaseous emissions and PM has also been investigated [28-30]. The temperature increase late in the combustion cycle due to the post-fuel injection, which can enhance soot oxidation, produced during the main combustion event [30-34], but this is reported to be dependent on the engine calibration and operation conditions. Some studies have reported PM increase with post-injection at high engine loads and speeds [28]. In some cases post-injection also contributes in the reduction of engine out NO_X due to the formation of nitrated-hydrocarbons through the reactions of NOx with HC radicals [35, 36]. It is reported that CO and THC are reduced with post-injection and sharply increased with later post-injection timing (after 70 CAD ATDC) [27]. Late combustion caused by post-injection increases the level of THC emissions as the late injected fuel is not burnt in the combustion chamber [26, 29, 37]. In this way, HCs are oxidized in the DOC, increasing considerably the temperature of the exhaust upstream of the DPF and trapping a high proportion of the soot flowing in the exhaust stream [27, 38, 39]. It is documented that the main-post-injection increases the rate of soot oxidation in the combustion cycle due to the enhancement of the gas mean temperature and air/fuel mixing, which leads to the reduction in number and diameter of primary particles [40, 41].

Combined advances in alternative fuels and aftertreatment systems are required in order to fulfil the stringent emission regulations and also help in decoupling mutual dependences between pollutants control and engine fuel economy. Most of the studies on alternative fuels combustion published in the literature are focused on the effect of the fuel on the engine performance and on the engine emissions, including PM characteristics [17] which influences passive and active DPF regeneration [20] as well as DPF trapping efficiency [42, 43]. Recent studies have reported work on gaseous emissions interactions [22] and the influence of PM characteristics [16] (size and shape) emitted from the combustion of different fuels on the DOC performance. However, there is still scarce information regarding the effect of alternative fuels (e.g. alcohol blends) on both, PM characteristics and DOC activity with simultaneous use of fuel post-injection, strategy that is required in diesel vehicles for catalyst heat-up in active and DPF regeneration. Therefore, the aim of this research work focuses on the role of the fuel post-injection and diesel-butanol fuel blends combustion on PM characteristics (number, size, morphology) and the impact on the DOC activity. The DOC catalyst activity was assessed under the same temperature, space velocity and pressure conditions with the only comparative parameter being the exhaust gas composition.

2. Experimental setup and materials

A modern single-cylinder, water-cooled, common rail fuel injection system, four-stroke experimental diesel engine was employed in this investigation. The engine used in this study is a single cylinder research engine that was designed by the investigators and incorporates one of the cylinder heads of a V6 production engine. The main specifications of the test engine can be found in Table 1. A schematic diagram of the experimental set up is shown in Figure 1. The diesel oxidation catalyst studies were carried out using one inch in diameter monolith catalyst that was placed in a reactor inside a furnace where the temperature and the engine exhaust gas flow can be controlled by a thermocouple (located upstream the catalyst) and a flow meter respectively.

Table 1. Research engine specifications.

Engine parameters	Specifications
Engine type	Diesel 1- Cylinder
Stroke Type	Four-Stroke
Cylinder Bore x Stroke (mm)	84 x 90
Connecting Rod Length (mm)	160
Compression Ratio	16.1
Displacement (cc)	499
Engine Speed Range (rpm)	900 – 2000
IMEP Range (bar)	< 7
Fuel Pressure Range (bar)	500 – 1500
Number of Injections	3 injection events

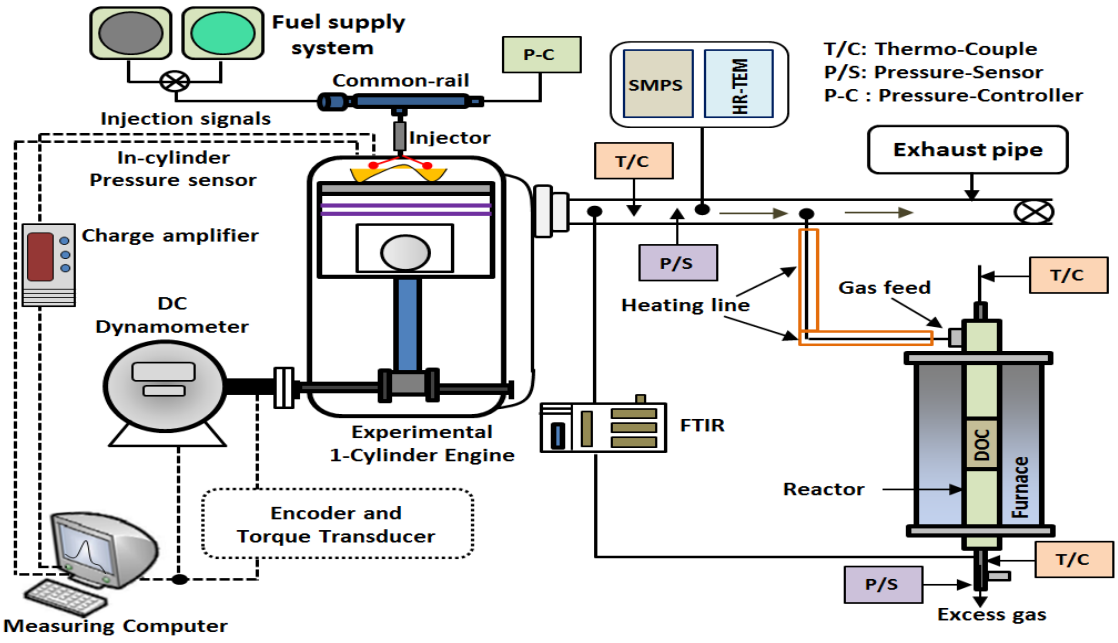

Figure 1. Schematic diagram of test platform and sampling system.

The Ultra Low Sulphur Diesel (ULSD) fuel used for the study was supplied by Shell Global Solutions UK. Butanol was purchased from Fisher Scientific Company and used in this study for the

diesel-butanol blends. The ULSD, butanol and fuel blend properties are presented in Table 2. The particular diesel fuel used in this research as reference fuel was selected without any biodiesel (thereby with zero oxygen content) in its composition, in order to study the effect of the oxygen in the combustion process when diesel fuel is blended with butanol. The diesel-butanol blend (B20) is a mix of 80% diesel and 20% butanol (%Vol.).

Table 2. Fuels specification [4, 16].

Properties	Method	ULSD	Butanol	B20D80
Cetane number	ASTM D7668-14	50.2	17	41.98
Latent heat of vaporization (kJ/kg)		243	585	-
Bulk modulus (MPa)		1410	1500	-
Density at 15 °C (kg/m^3)	EN 12185	840.4	809.5	833.2
Upper heating value (MJ/kg)		45.76	36.11	43.5
Lower heating value (MJ/kg)		43.11	33.12	40.91
Water content by coulometric KF (mg/kg)	EN 12937	40	170	389.4
Kinematic viscosity at 40 °C (cSt)	EN ISO 3104	2.564	2.23	2.27
Lower Calorific Value (MJ/kg)		43.11	33.12	39.95
Lubricity at 60 °C(μm)	EN ISO 12156	424	571.15	444.5
Fatty acid methyl ester % (v/v)	NF EN 14078-A	<0.05		
Cold filter plugging point (CFPP)	ASTM D-6371	-18	<-51	-18
C (wt %)		86.44	64.78	81.56
H (wt %)		13.56	13.63	13.35
O (wt %)		0	21.59	4.318

At significantly lower or higher that 300 °C exhaust gas temperatures; the impact of fuels and post injection strategy on the DOC may not be as robust and conclusive as the catalyst may not light-off (low load) or the activity may not be affected (high loads). All tests were performed under a constant engine speed of 1800 rpm with an engine load of 3 bar IMEP (Indicated Mean Effective Pressure). An AVL GH13P was used to record the in-cylinder pressure [44]. The charge from the pressure transducer (mounted in the cylinder head) was amplified by an AVL FlexiFEM 2P2 Amplifier [45]. A digital shaft encoder producing 360 pulses per revolution was used to measure the crank shaft position. The data from the crank shaft position and pressure was combined to create an in-cylinder pressure trace. The engine is equipped with common-rail fuel injection system which allows the control of multiple injection events. The injection was split in pre, main, and post fuel injection with injection timing of 15 and 3 deg bTDC and 60 deg aTDC, injection pressure of 650 bar, and post-injection duration of 0.1 ms. A bespoke experimental facility was used in this study that was designed to assess the performance of catalysts and combination of aftertreatment systems under real engine exhaust gas while providing flexibility with temperatures and reductants (i.e. hydrocarbons, ammonia, hydrogen) selection. The DOC used in this study was supplied by Johnson Matthey Plc and was positioned inside a mini reactor that was located inside a furnace and was fed with real engine exhaust

gas. The temperature upstream the DOC was monitored using K-type thermocouples. The temperature of the reactor inside a tubular furnace was set at 300 °C while maintaining constant gas hourly space velocity (GHSV) of 35000 h^{-1}. The details of the catalyst (DOC) used in this study was a 4.237 kg/m^3 with optimal platinum:palladium proportion (weight ratio 1:1) with alumina and zeolite washcoat (158.66 kg/m^3 loading). The total dimensions of the DOC were 25.4 mm diameter, 91.4 mm length, and 4.3 mil wall thickness of the DOC [16, 22, 23].

A MultiGas 2030 FTIR spectrometry based analyzer was employed for exhaust gaseous emissions measurement such as: carbon monoxide (CO), carbon dioxide (CO_2), nitrogen oxide (NO and NO_2), nitrous oxide (N_2O), and individual hydrocarbons species such as methane (CH_4), ethane (C_2H_6), ethylene (C_2H_4). Particulate Size Distributions (PSD) were analysed using a TSI 3080 scanning mobility particle sizer (SMPS). Exhaust gas part was sampled and diluted with air when using the rotating disk thermodiluter (TSI 379020A) to control the dilution ratio. The dilution ratio was set at 1:100 for all the tests and the thermodiluter temperature was 150 ˚C. The SMPS was connected downstream of the dilution system in order to extract a diluted sample for the particle size measurement.

Soot particles were collected from the exhaust pipe on a 3.05 mm diameter copper grids attached to a sampling probe. The sampling tool and lines were cleaned with nitrogen before each test to remove deposited soot particles. A Philips CM-200 high resolution transmission electron microscopy (HR-TEM) with a resolution about 2 Å at an accelerating voltage of 200 kV was used to analyse the particles. A digital image analysis software in Matlab was designed to calculate the morphological parameters of the agglomerates (radius of gyration, R_g, number of primary particles, n_{po}, and fractal dimension, D_f) [46, 47]. The conversion from pixels to nanometres was calibrated by comparison with standard latex spheres shadowed with gold. For each condition, two grids and minimum 33 photographs were taken per fuel to calculate the morphology parameters as well as least 26 agglomerates were chosen for each condition and fuel to obtain the results. Furthermore, more than 200 primary particles were manually and randomly selected from different aggregates to determine an average diameter of primary particles and to produce the fitted normal distribution of primary particles at each fuel and condition.

3. Results and discussions

3.1 Combustion characteristics

Figure 2 shows the effects of the injection strategy on the in-cylinder pressure and the rate of heat release (ROHR) versus crank angle degree (CAD) for the combustion of diesel and B20. It has to be noted that neither the post-injection nor the fuel properties notably affected the combustion events. It is though that this is due to the effect of the pre-injection which thermally conditioned the in-

cylinder, thus minimizing the effect of the worse autoignition properties (Table 2) of the B20 blend with respect to diesel fuel. Small increase of the in-cylinder pressure and heat release was obtained from the combustion of B20 that may also explain the changes in emissions later on.

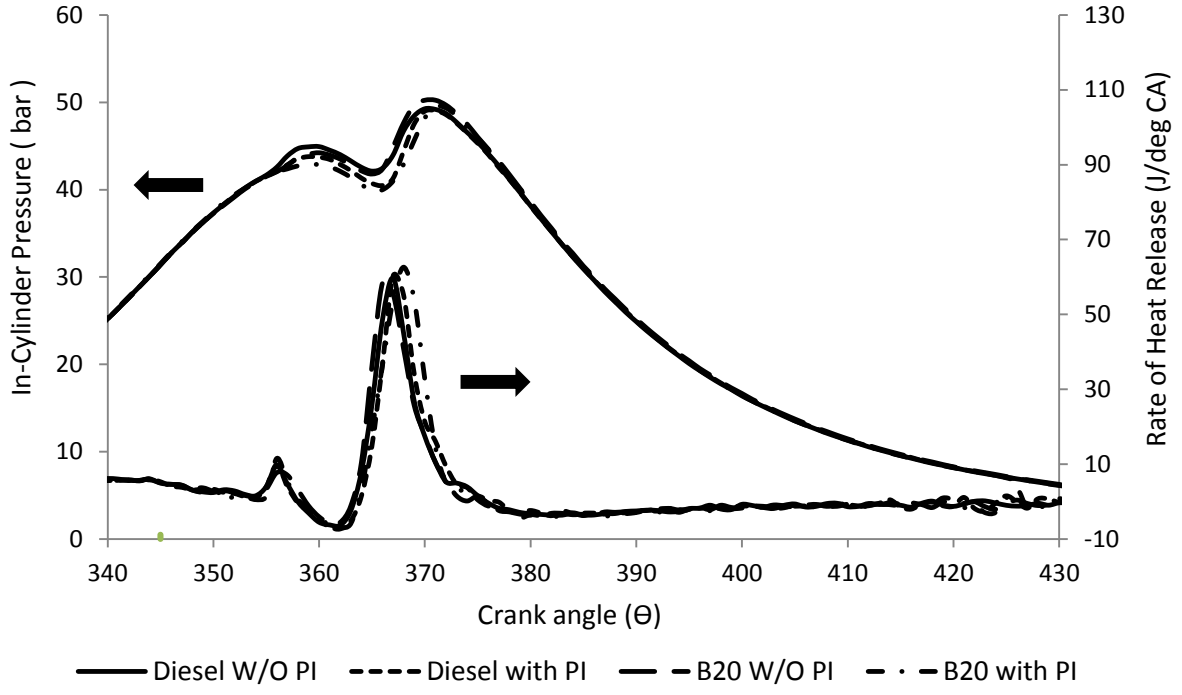

Figure 2. Effect of fuel post-injection strategy and fuels structure on combustion characteristics.

3.2 Influence of fuel post-injection and fuel structure on engine out PM and gaseous emissions

The PSDs were obtained upstream the DOC in order to understand the influence of B20 and post-injection on the particle formation and oxidation processes. The combustion of the alcohol blend (B20) reduced the number of particles along the whole distribution with respect to combustion of the diesel fuel with and without post-injection (Figure 3). A slight reduction is observed in the average particle diameter, from 94 nm for diesel down to 64 nm for B20 in the absence of post-injection. These results are in agreement with previous studies of butanol-diesel blends combustion [16, 48] justified by the presence of the hydroxyl group in the butanol molecule [16] leading to lower rates of PM formation [4, 16] and to enhanced PM oxidation rates [16, 49]. Reductions of the soot in the exhaust are often reported when post-injection is introduced due to increased expansion temperature and enhanced mixing within the cylinder that increases oxidation of soot produced from the main injection [30, 32-34].

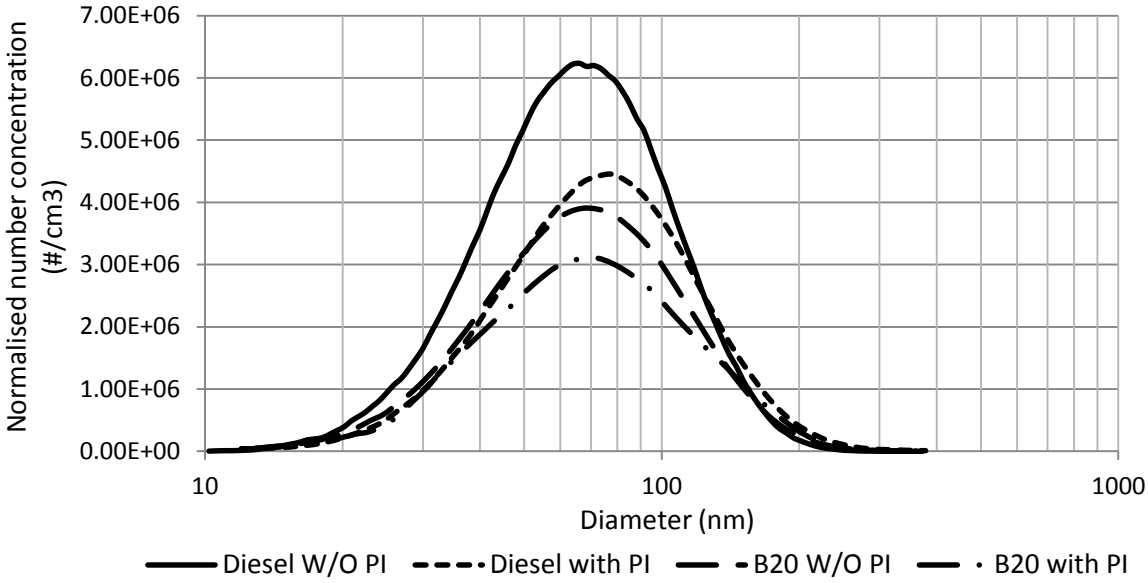

188

189 **Figure 3.** Effect of post-injection on particle size distribution for diesel and B20 fuels**.**

190 The particles emitted from diesel engine have a variety of shapes and sizes and consist of tens
191 to hundreds of primary particles agglomerated together, forming irregular clusters [50, 51]. Figure 4
192 depicts representative examples of HR-TEM micrographs from particles sampled from the exhaust
193 gas at the different conditions studied in this research. PM morphological parameters (radius of
194 gyration (R_g), number of primary particles (n_{po}) and fractal dimension (D_f)) for Diesel and B20 are
195 calculated from the obtained HR-TEM images. Figure 5 shows the results of the average particles
196 electrical mobility diameter obtained with SMPS jointly with soot's average radius of gyration and
197 number of primary particles. According to these results the average agglomerate size (quantified by
198 radius of gyration and mobility diameter) and the number of primary particles are lower for B20 than
199 for diesel fuel independently of the injection strategy. It is believed that for diesel combustion the
200 enhanced net formation rate of particles increases the likelihood of collisions and further aggregation
201 leading to higher number of primary particles. It is thought that oxygen content in butanol blend (B20)
202 improves the soot oxidation [52] while the incorporation of the post-injection leads to enhanced
203 oxidation resulting in the disappearance of a fraction of the primary particles already formed (Figure
204 5). The reduction in number of particles as measured by the SMPS and the reduction in number of
205 primary particles in the particle aggregate for B20 are also associated with the reduction in the
206 formation of soot precursors due to the chemical structure of butanol and the lack of PAH in butanol,
207 besides the effect of the oxygen content of butanol.

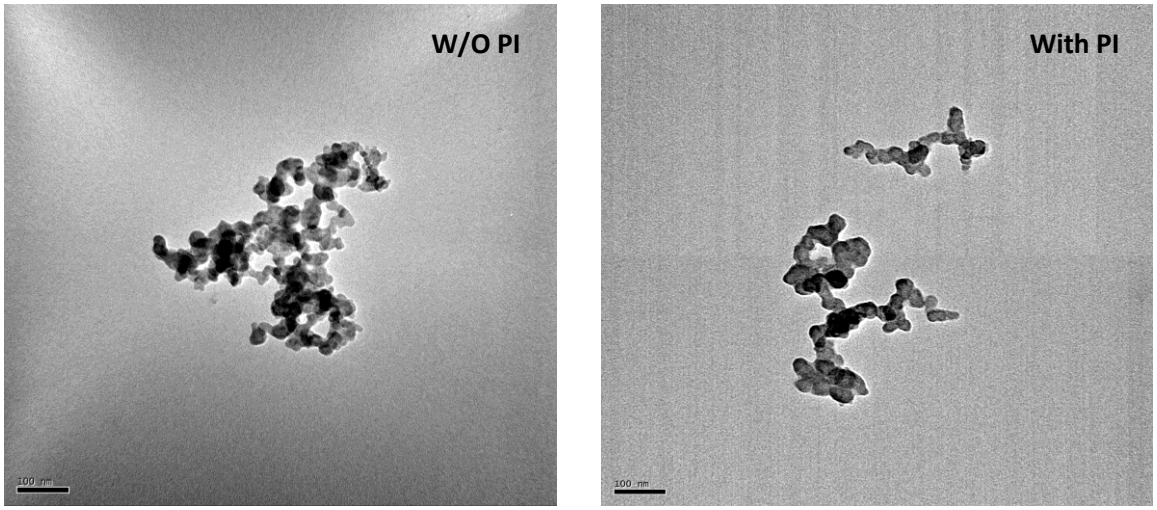

(a)

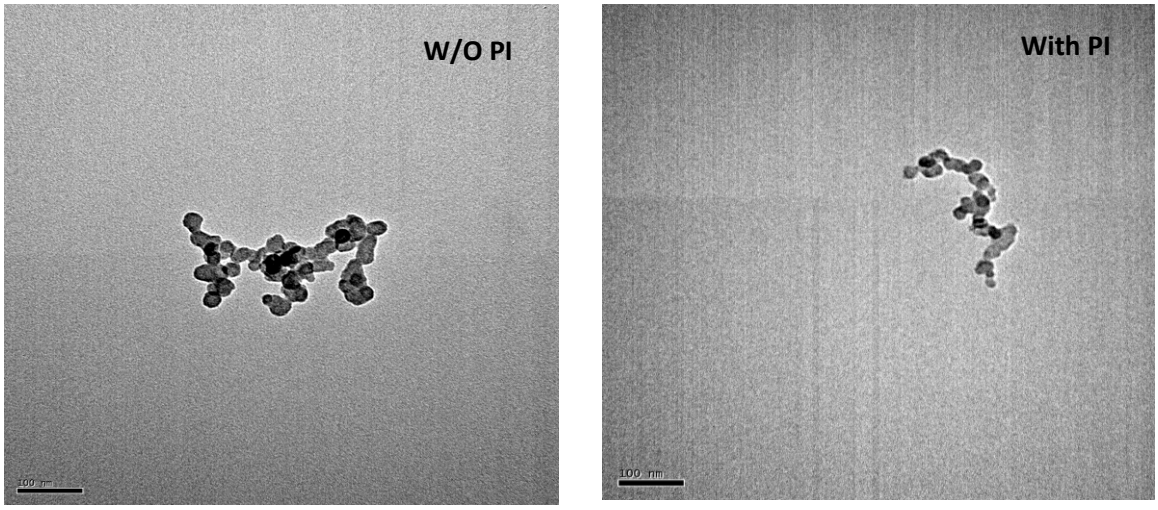

(b)

208 **Figure 4.** Typical examples of HR-TEM micrograph of particles matter collected at the exhaust gas
209 for (a) diesel fuel, and (b) B20.

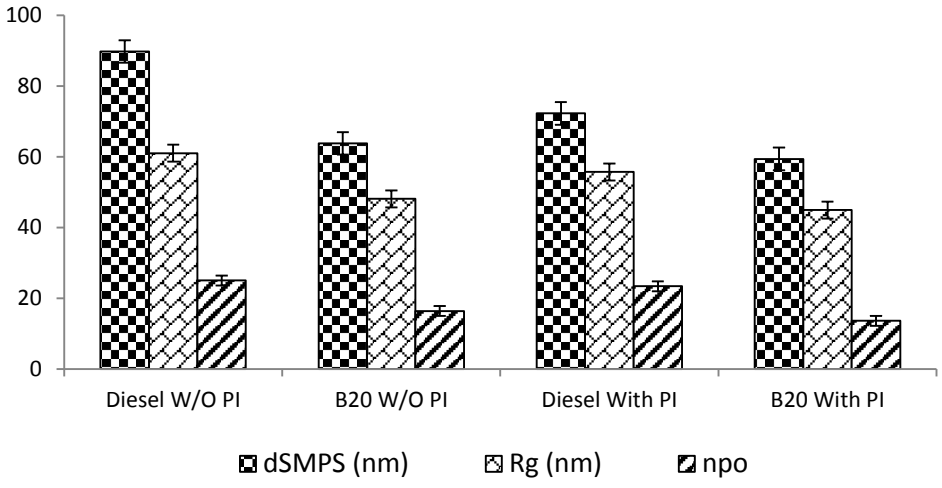

210

211 **Figure 5.** Effect of fuel injection strategy and fuel characteristics on particle size from SMPS, radius
212 of gyration (R_g) and number of primary particles (n_{po}).

The influence of the fuel and injection strategy (with and without post-injection) on the fractal dimension (D_f) is shown in Figure 6. The fractal dimension of the agglomerates produced from the diesel fuel is higher (by 1.62-1.66) than that from B20 for both injection strategies (Figure 6) and this is in agreement with the work described by both Fayad et al. [16] and Choi et al. [53]. As a general rule a reduction of the fractal dimension should be expected when there is a high concentration of particles as a result of the increased likelihood of collisions between agglomerates. However, in the case of agglomerates from oxygenated fuels, despite the lower particle concentration (and the consequent reduced likelihood of collisions) fractal dimensions were not found to be higher, but were systematically lower instead, probably due to some internal oxidation of agglomerates occurring after being formed. Similarly, the fractal dimension is also lower when post-injection was introduced for both fuels, despite the higher particle concentration also in this case (Figure 6). A conceptual model is suggested here to justify these trends. In the early stage of nuclei and primary particle formation fractal dimension is close to 3 and the primary particle size continuously increases (spherical nuclei and spherical primary particles). Collisions between particles and agglomerates and between agglomerates and agglomerates will increase the size of the agglomerate and reduce their fractal dimension (particle growth dominant over particle oxidation). This phenomenon will be more intense in the case of diesel without post injection conditions due to the higher rate of particle formation. Afterwards, the oxidation of particles will become dominant over the particle formation and the size of both primary particles and agglomerates could decrease, while the fractal dimension will deeply decrease, for the reason pointed out above. In this case, the decrease in fractal dimension will be more intense for the case of oxygenated fuels and post-injection conditions. Therefore, it is speculated that the resultant agglomerates from oxygenate fuels and post-injection conditions will have lower fractal dimension as the oxidation will remain being the dominant mechanism in front of particle formation and growth for longer time, as a consequence of the enhanced reactivity of soot particles (in the case of oxygenated fuels/) or of the enhanced temperature conditions in the exhaust flow (in the case of post-injection). More research and some in-cylinder sampling techniques should be used for a more comprehensive justification.

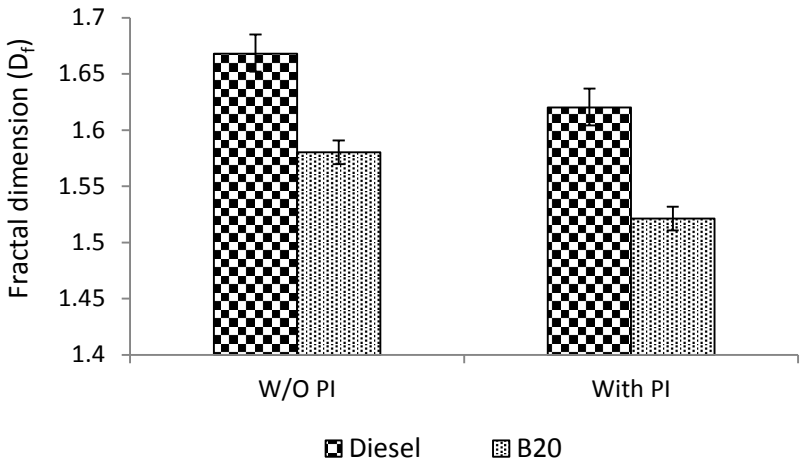

240

241 **Figure 6.** Fractal dimensions of particulate matter from the HR-TEM images.

242 The primary particle diameter (d_{po}) size distribution for both fuels with or without post-
243 injection has been measured by selecting around 200 primary particles (more than 33 HR-TEM
244 photographs for each condition and fuel) in order to fit normal distribution as shown in Figure 7. Figure
245 8 shows smaller size primary particles from the combustion of B20 for both injection setting (with and
246 without post-injection) compared to diesel primary particles due to lower rate of production of soot
247 precursors, soot formation and soot growth, and to the increase soot oxidation during the combustion
248 of oxygenated fuel [16]. This result is in agreement with results obtained from biodiesel fuel [54] and
249 butanol [16, 55] fuel blends without post-injection using other engine technologies [16, 55]. The size
250 of primary particles is slightly reduced when post-injection was used for both fuels (Figure 8). It is
251 believed this is due to an enhancement in the soot oxidation rate in the expansion stroke under post-
252 injection conditions.

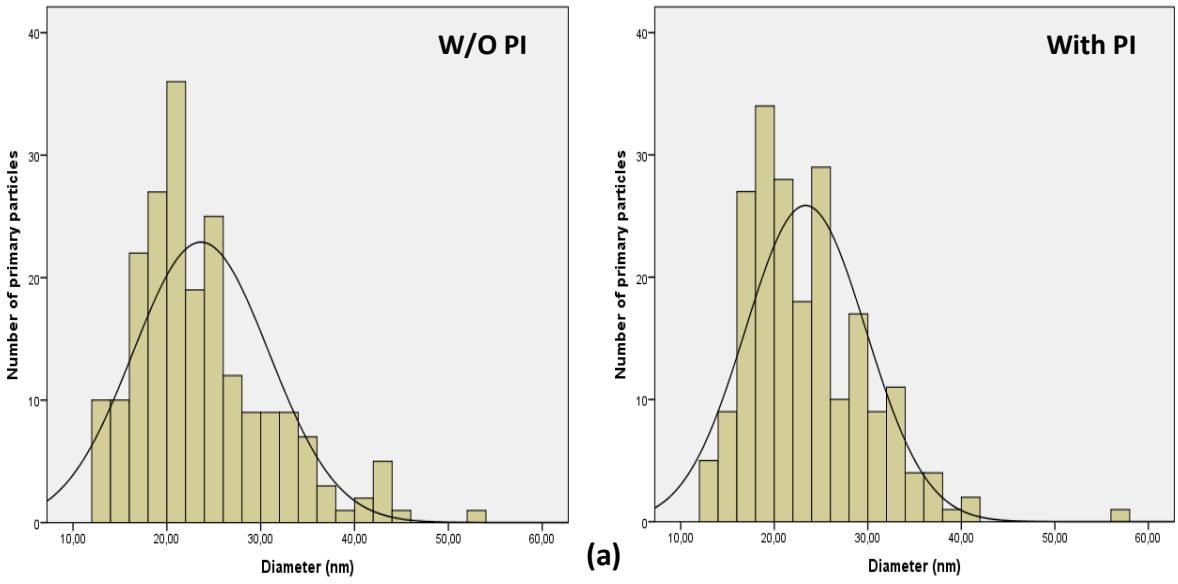

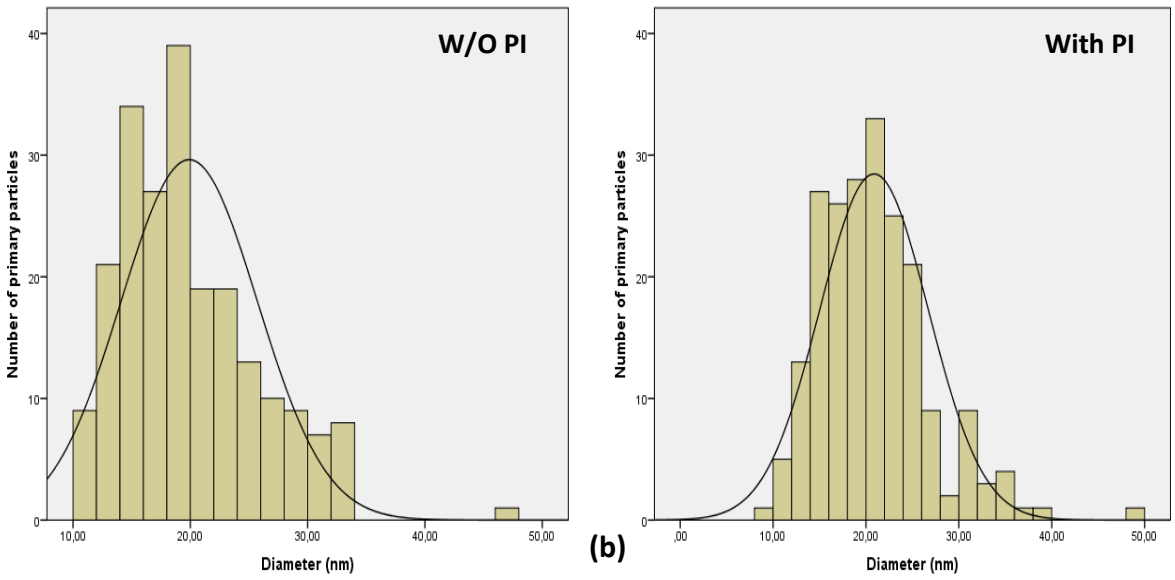

253 **Figure 7.** Primary particles size distributions for (a) diesel fuel, and (b) B20.

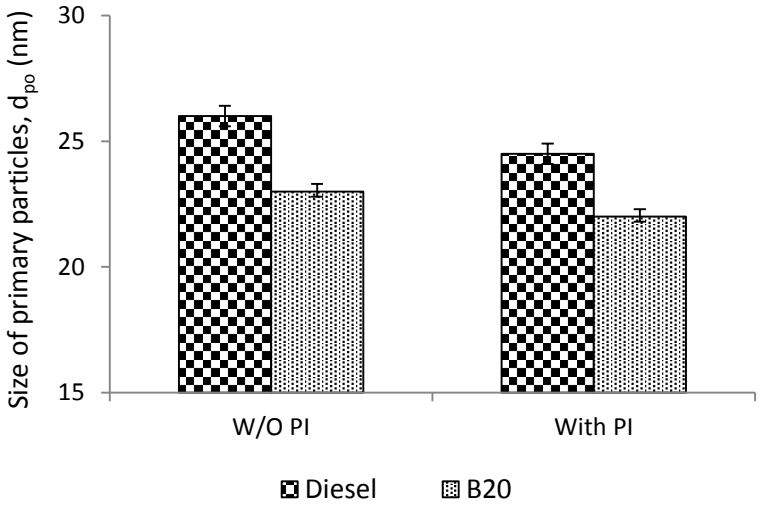

254

255 **Figure 8.** Average size of primary particles (d_{po}) for diesel and B20.

256 Figure 9 shows the CO, heavy HC, and THC engine-out emissions for the two studied fuels at
257 both injection strategies. It can be noticed that THC emissions were lower from the combustion of the
258 alcohol blend (B20) for both injection strategies. The higher HC emissions observed with diesel can
259 be attributed to several reasons including absence of oxygen in the fuel molecule, and less efficient
260 oxidation. The THC emissions in the case of post-injection are much higher compared to the case
261 without post-injection. This confirms that the quantity and timing chosen for the post-injection allows
262 to keep most of them unburnt and available to be oxidised in the DOC. Yamamoto, et al. and Chen,
263 [26, 30] reported that the late post-injection lead to high level of THC emissions. It is reported that the
264 reason of the increase in CO emissions observed for B20, especially without post-injection, can be

attributed to the expected lower local in-cylinder temperature (Figure 2) and less CO oxidation during the combustion process due to the higher enthalpy of vaporisation of butanol with respect to diesel fuel [27]. Therefore, it seems that at this engine load operation the oxygen content and high reactivity of the butanol molecule enables to partially oxidise most of the HC species to CO, but the colder in-cylinder conditions due to the enthalpy of vaporization of butanol hinders the complete oxidation from CO to CO_2.

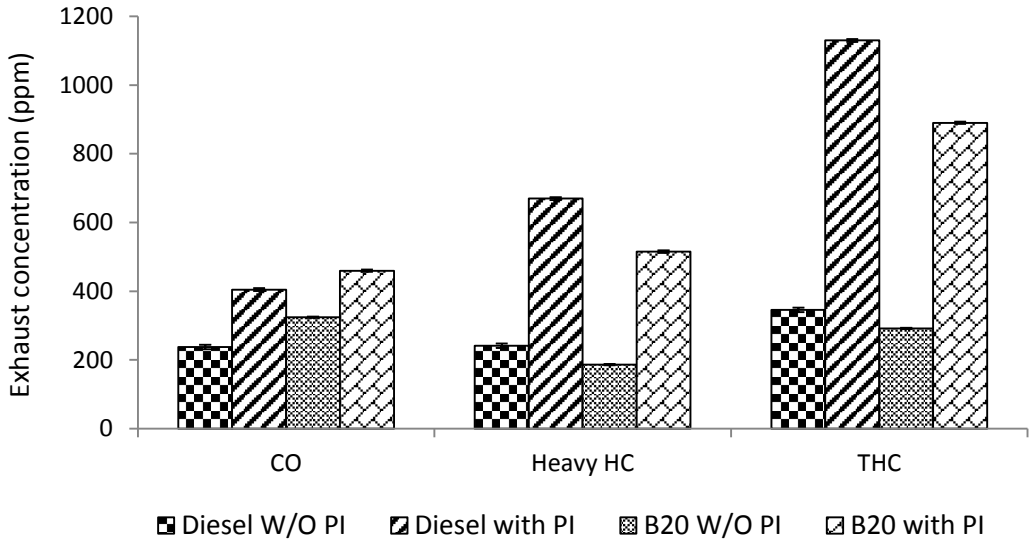

Figure 9. Engine exhaust gaseous emissions.

The concentration of HC species in the engine exhaust upstream the catalyst differs for diesel and B20 engine fuelling (Figure 10). The concentration of the light HC species studied including saturated (methane, ethane) and unsaturated (ethylene) species is higher for B20 with respect to diesel fuel combustion, conversely to the THC emissions presented earlier. It is thought that this is due to the thermal decomposition of the butanol component to light HC species and CO rather than forming heavy HC components as in the case of diesel fuel combustion. The level of HC emissions was lower from the combustion of B20 compared to the diesel fuel combustion. This can be due to improved combustion efficiency of the fuel in the presence of oxygen in the fuel as has also been described in [56] and due to the combustion patterns described in Figure 2, where a small increase in the in-cylinder pressure was obtained. From the results it can be also observed that with the incorporation of the fuel post-injection, higher concentration of the total and selected HC species were measured for both fuels due to the late timing of the post-injection [26].

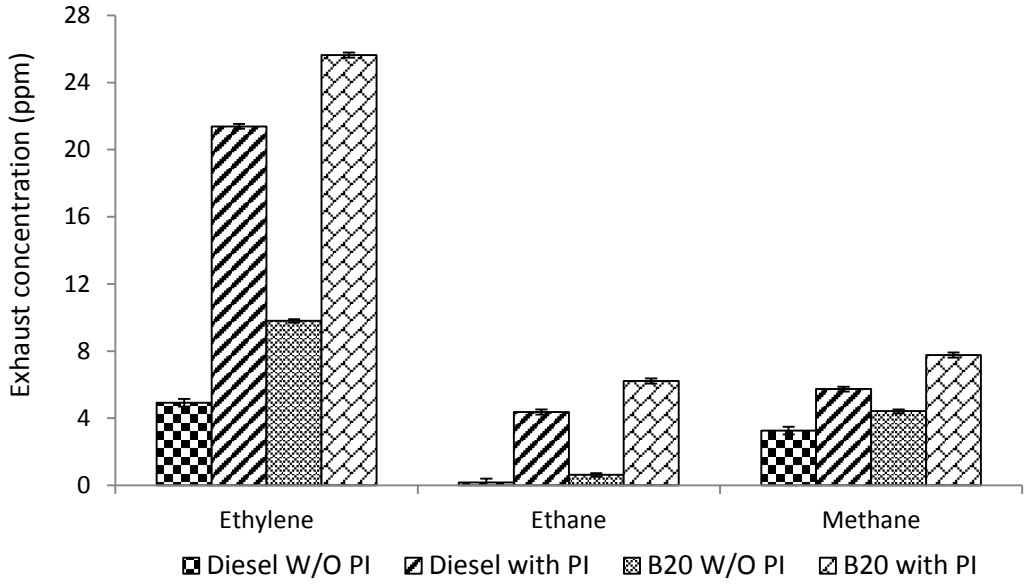

Figure 10. Engine exhaust hydrocarbon species measured upstream the DOC.

A slight increase in NO_X ($NO + NO_2$) was measured for the B20 combustion with respect to diesel combustion for both injection strategies (Figure 11). This can be due to the slight increase of in-cylinder pressure as seen in Figure 2 and the presence of the chemically bound oxygen content in B20 as it has been previously reported in the case of oxygenated fuels [56]. In addition, the oxygen content and lower cetane number of butanol enhanced the burning rate (faster burning). Chen et al [57] reported similar trends in NOx emissions from the combustion of n-butanol-diesel blends and suggested that this was a result of the ignition delay that was then led to wider high-temperature combustion region. Although both fuels have similar NO concentration, it seems that B20 blend has higher oxidation from NO to NO_2 than diesel fuel due to the oxygen in the molecule. When post-injection was utilised the emissions of NO were decreased with simultaneously increasing in NO_2 for both fuels (Figure 11). This is can be explained because a portion of NO was oxidised to NO_2 by hydroperoxy radical (HO_2) formed during post combustion [58] and because of the reduction of NO_X with some of the HCs post-injected. It was noted that the engine out NO_x emissions decreased under post-injection due to the possible formation of nitrated-hydrocarbon by reacting NO_x with radical HC [58].

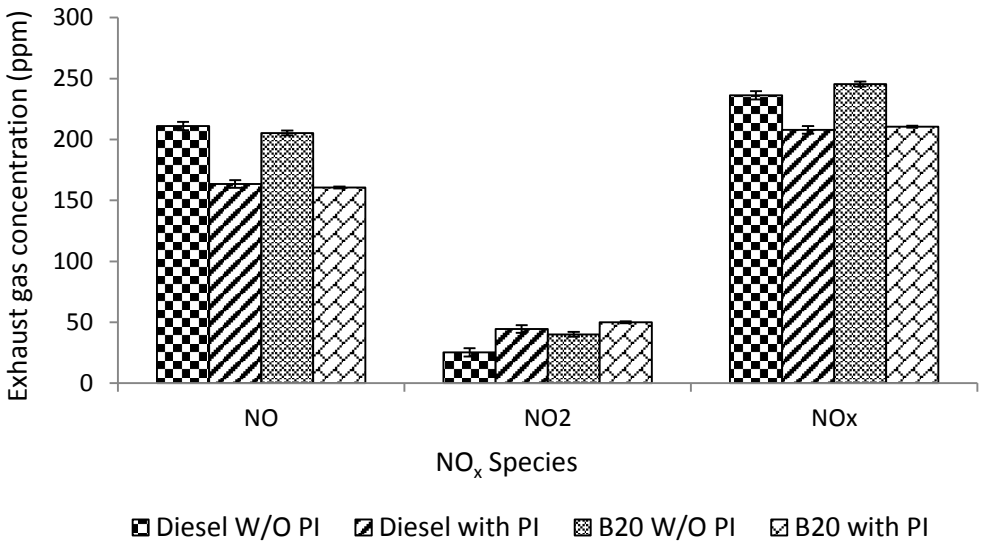

Figure 11. NO_X species concentrations of each gas species for with and without post-injection.

3.3 Brake specific fuel consumption and brake thermal efficiency

The brake specific fuel consumption (BSFC) and brake thermal efficiency (BTE) for both diesel and butanol blends are summarized in Table 3. It was noticed that post injection strategy increased the brake specific fuel consumption (BSFC) compared to that of main injection for both fuels. Moreover, BSFC slightly increased with B20 for both injection strategies when compared to the diesel fuel. The mean increase in BSFC for B20 when compared to the diesel under the same condition is 0.02811 and 0.02903 kg/kWh for without post-injection and with post-injection respectively. This is due to the lower calorific value recorded for B20 (see Table 2) compared to the diesel fuel. Lapuerta et al. [59] and Hajbabaei et al. [60] reported that the oxygenated fuels increases the BSFC mainly due to the reduced calorific value when compared to the diesel. Furthermore, the smaller increase in BSFC for B20 its compensated by its lower calorific value resulting in an increase in brake thermal efficiency efficiency. This could be due to the oxygen content in the B20 which leads to improving the combustion and this consistent with other researchers cited in introduction. It is clear from Table 3 that the post-injection reduces brake thermal efficiency and increase the exhaust gas temperature (EGT) for both fuels.

Table 3. Brake specific fuel consumption and thermal efficiency.

Fuel	Diesel fuel		B20	
Parameters	W/O PI	With PI	W/O PI	With PI
Brake specific fuel consumption, BSFC (kg/kWh)	0.3484	0.3645	0.3765	0.3935
Exhaust gas temperature, EGT (°C)	283	291	272	284
Brake thermal efficiency (BTE)	23.97	23.25	25.44	24.83

3.4 Influence of fuel post-injection and fuel properties on DOC activity

Combustion by-products in the exhaust gas are competing with each other to be adsorbed into the active sites of the catalyst [16, 22], effects that is highly depends on the temperature, flow conditions, space velocity and concentration and nature of the exhaust species. In active control aftertreatments such as diesel particulate filters (DPFs) the ability of the DOC to effectively oxidise the fuel and hydrocarbons and provide the required heat is important for the efficient operation of the engine system (including aftertreatment and engine fuel economy and emissions). The gas hourly space velocity (GHSV) and temperature of the DOC in this study were controlled and set at 35000 h^{-1} and 300 °C, respectively in order to isolate the effect of exhaust gas composition.

The DOC is very effective in reducing CO in the engine exhaust from the combustion of both fuels, with the catalyst's CO conversion efficiency being higher for B20 blend. In the case of post-injection, the catalyst's CO oxidation efficiency was reduced (Figure 12), this is due to increased concentration of species that are now competing for the same number of active sites. The HC species presented in Figure 12 are light saturated (methane, ethane), light unsaturated (ethylene) and heavy HCs. The results confirm the differences in reactivity of the hydrocarbon species. Methane (CH_4) as a short chain saturated hydrocarbon was the most difficult component to oxidise in the catalyst due to its low oxidation reactivity [23, 61]. Particularly, it can be observed that the conversion efficiency of methane over the catalyst was even lower than 10% at 300 °C for all the conditions studied. In addition, the increased concentration of heavier HCs and fuel in the exhaust that reaches the DOC leads to its non-selective poisoning (i.e. fouling or masking). The catalyst active sites are now occupied by the increased concentration of HCs and fuel that are interfering with the reactants transport phenomena to the catalyst active sites. This non-selective poisoning limits the catalytic surface area and obstructs access of the reactants to the pores. In this case the effect is reversible as for the B20 fuel combustion, the catalyst has the highest HC conversion efficiency at 300 °C compared with diesel fuel (Figure 12). This could be due to several reasons such as lower concentration of HC upstream the catalyst, higher reactivity of butanol and its derivatives, higher level of NO_2 emissions to catalytically oxidise the HC species [16, 62], lower PM/soot levels that can be responsible for blocking the active sites.

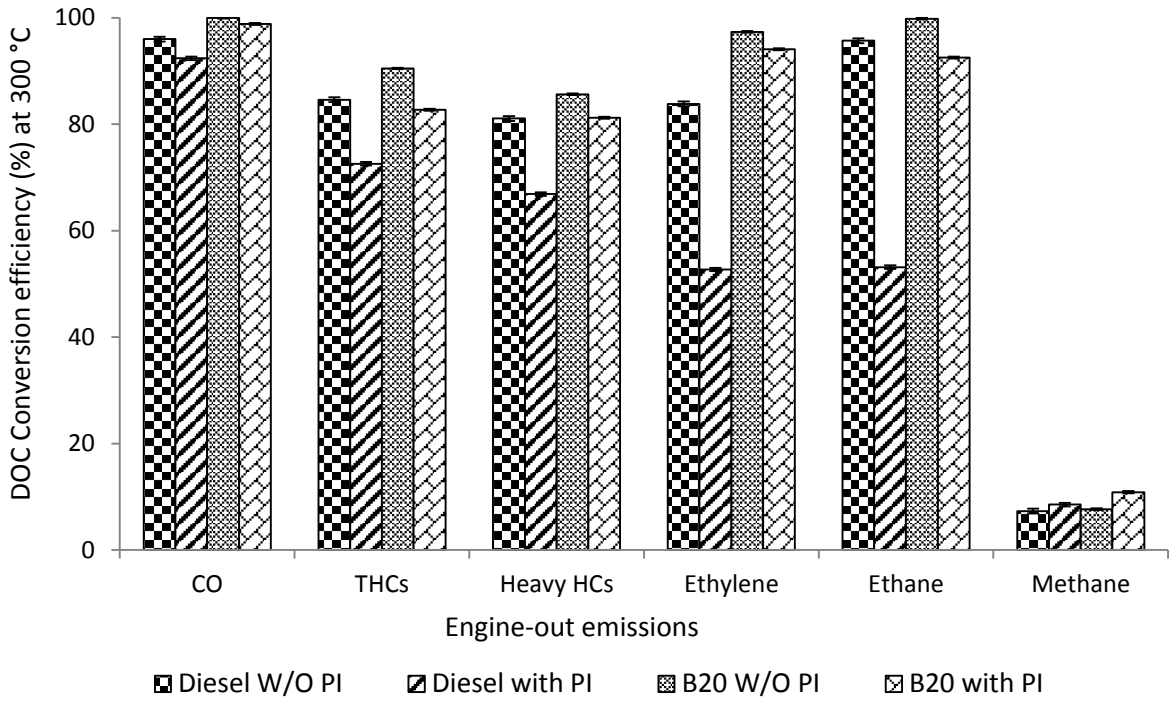

346

347 **Figure 12.** DOC activity at 300 °C.

348 ## 4. Conclusions

349 The effect of fuel post-injection and butanol-diesel fuel blends (B20) on PM characteristics
350 (including size, fractal dimension, radius of gyration, and size of primary particles) and gaseous
351 emissions were analysed and their influence on DOC activity was investigated at exhaust temperature
352 of 300 °C. Due to reduced PM number concentration and HC emissions from the combustion of B20
353 the catalyst activity was improved. The HR-TEM analysis showed that the number of primary particles
354 of PM agglomerates emitted from B20 combustion was lower than that from the combustion of diesel
355 fuel. As B20 has oxygen-containing compounds, they contribute to inhibit the rate of soot formation
356 and to increase the rate of oxidation, resulting in particles with smaller average size and fractal
357 dimension. It is observed that the fuel post-injection has more clear benefits on PM reduction, resulting
358 in enhanced soot oxidation with similar trends on the morphology of agglomerates as the presence of
359 oxygenated compounds. HR-TEM analysis supports the results from SMPS and revealed that B20
360 produces particles with smaller average size compared to diesel fuel.

361 The fuel components as has been highlighted from the use of primary alcohols in this study,
362 can improve engine systems performance by providing a chain of beneficial effects; from the
363 combustion process to emissions formation processes to their abatement processes in the
364 aftertreatment systems. In this case the changes in fuels properties from the incorporation of butanol
365 into diesel fuel, led to cleaner combustion that eased species (i.e. HCs/fuel and engine out emissions)

oxidation in the DOC. These trends will favour the active control strategies in the aftertreatment systems and will positively impact on their performance (i.e. increase activity, improve durability) and overall engine fuel economy.

5. Acknowledgements

Special thanks to the to the Iraqi government and Ministry of Higher Education and Scientific Research in Baghdad, Iraq for providing PhD scholarship and maintenance grant for M.A. Fayad. Innovative UK (*The Technology Strategy Board*, TSB) and EPSRC (*Engineering and Physical Science Research Council*) acknowledged for funding/supporting this work with the projects CREO ref 400176/149 and EP/G038139/1, respectively. Johnson Matthey is acknowledged for providing the catalysts. F.J. Martos expresses thanks to the government of Spain for supporting his research stay with reference PRX15/00256 at University of Birmingham. D. Fernández-Rodríguez expresses thanks to the University of Castilla-La Mancha (Spain) for supporting his research stay at the University of Birmingham. With thanks to Advantage West Midlands and the European Regional Development Fund, funders of the Science City Research Alliance Energy Efficiency project-a collaboration between the Universities of Birmingham and Warwick.

ABBREVIATIONS

aTDC = after top dead centre
B20D80 = butanol 20 %, and diesel 80%
bTDC = before top dead centre
BSFC = brake specific fuel consumption
CAD = crank angle degree
CI = compression ignition
CO = carbon monoxide
CO_2 = carbon dioxide
d_{po} = size of primary particles
DOC = diesel oxidation catalyst
DPF = diesel particulate filter
EGT = exhaust gas temperature
GHSV = gas hourly space velocity
HC = hydrocarbons
IMEP = indicated mean effective pressure
NO = nitric oxide
NO_2 = nitrogen dioxide
NO_X = nitrogen oxides
n_{po} = number of primary particles

R_g = radius of gyration

SMPS = scanning mobility particle sizer

PSD = particulate size distribution

PI = post-injection

PM = particulate matter

TEM = transmission electron microscopy

THC = total hydrocarbons

ULSD = ultra low sulfur diesel

M-I = main injection

W/O PI = without post-injection

BTE = brake thermal efficiency

6. References

1. Bouchez, M., Dementhon, J. B., *Strategies for the control of particulate trap regeneration*. 2000, SAE technical paper.
2. Gill, S.S., Chatha, G. S., Tsolakis, A., *Analysis of reformed EGR on the performance of a diesel particulate filter.* international journal of hydrogen energy, 2011. **36**(16): p. 10089-10099.
3. Zhu, L., Z. Huang, and J. Fang, *The Effects of Diesel Oxidation Catalyst on Particulate Emission of Ethanol-Biodiesel Blend Fuel*. 2014, SAE Technical Paper.
4. Sukjit, E., Herreros, J. M., Dearn, K. D., Garcia-Contreras, R., Tsolakis, A., *The effect of the addition of individual methyl esters on the combustion and emissions of ethanol and butanol - diesel blends.* Energy, 2012. **42**(1): p. 364-374.
5. Koivisto, E., Ladommatos, N., Gold, M., *Systematic study of the effect of the hydroxyl functional group in alcohol molecules on compression ignition and exhaust gas emissions.* Fuel, 2015. **153**: p. 650-663.
6. Zhang, Z., Balasubramanian, R., *Investigation of particulate emission characteristics of a diesel engine fueled with higher alcohols/biodiesel blends.* Applied Energy, 2016. **163**: p. 71-80.
7. Mwangi, J.K., Lee, W., Chang, Y., Chen, C., Wang, L., *An overview: Energy saving and pollution reduction by using green fuel blends in diesel engines.* Applied Energy, 2015. **159**.
8. Bermudez, V., Lujan, J.M., Pla, B., Linares, W.G., *Comparative study of regulated and unregulated gaseous emissions during NEDC in a light-duty diesel engine fuelled with Fischer Tropsch and biodiesel fuels.* Biomass and Bioenergy, 2011. **35**.
9. Lapuerta, M., Armas, O., Herreros, J.M., *Emissions from a diesel-bioethanol blend in an automotive diesel engine.* Fuel, 2008. **87**: p. 25-31.
10. Hellier, P., Ladommatos, N., Allan, R., Rogerson, J., *The Influence of Fatty Acid Ester Alcohol Moiety Molecular Structure on Diesel Combustion and Emissions.* Energy & fuels, 2012. **26**: p. 1912-1927.
11. Eveleigh, A., Ladommatos, N., Hellier, P., Jourdan, A., *An investigation into the conversion of specific carbon atoms in oleic acid and methyl oleate to particulate matter in a diesel engine and tube reactor.* Fuel, 2015. **153**: p. 604-611.
12. Xing-cai, L., Jian-Guang, Y., Wu-Gao, Z., Zhen, H., *Effect of cetane number improver on heat release rate and emissions of high speed diesel engine fueled with ethanol–diesel blend fuel.* Fuel, 2004. **83**(14): p. 2013-2020.
13. Zoldy, M., A. Hollo, and A. Thernesz, *Butanol as a diesel extender option for internal combustion engines*. 2010, SAE Technical Paper.

14. Armas, O., García-Contreras, R., Ramos, Á., *Pollutant emissions from New European Driving Cycle with ethanol and butanol diesel blends.* Fuel Processing Technology, 2014. **122**: p. 64-71.
15. Lapuerta, M., Armas, O., García-Contreras, R. , *Effect of Ethanol on Blending Stability and Diesel Engine Emissions.* Energy & fuels, 2009. **23**(9): p. 4343-4354.
16. Fayad, M.A., Herreros, J. M., Martos, F. J., Tsolakis, A., *Role of Alternative Fuels on Particulate Matter (PM) Characteristics and Influence of the Diesel Oxidation Catalyst.* Environmental science & technology, 2015. **49**(19): p. 11967-11973.
17. López, A.F., Cadrazco, M., Agudelo, A. F., Corredor, L. A., Vélez, J. A., Agudelo, J. R, *Impact of n-butanol and hydrous ethanol fumigation on the performance and pollutant emissions of an automotive diesel engine.* Fuel, 2015. **153**: p. 483-491.
18. Rakopoulos, D.C., Rakopoulos, C. D., Giakoumis, E. G., Dimaratos, A. M., Kyritsis, D. C., *Effects of butanol–diesel fuel blends on the performance and emissions of a high-speed DI diesel engine.* Energy Conversion and Management, 2010. **51**(10): p. 1989-1997.
19. Rakopoulos, D.C., Rakopoulos, C. D., Papagiannakis, R. G., Kyritsis, D. C., *Combustion heat release analysis of ethanol or n-butanol diesel fuel blends in heavy-duty DI diesel engine.* Fuel, 2011. **90**(5): p. 1855-1867.
20. Rounce, P., A. Tsolakis, and A. York, *Speciation of particulate matter and hydrocarbon emissions from biodiesel combustion and its reduction by aftertreatment.* Fuel, 2012. **96**: p. 90-99.
21. Ye, S., Yap, Y. H., Kolaczkowski, S. T., Robinson, K., Lukyanov, D., *Catalyst 'light-off'experiments on a diesel oxidation catalyst connected to a diesel engine—Methodology and techniques.* Chemical Engineering Research and Design, 2012. **90**(6): p. 834-845.
22. Lefort, I., Herreros, J. M., Tsolakis, A., *Reduction of low temperature engine pollutants by understanding the exhaust species interactions in a diesel oxidation catalyst.* Environmental science & technology, 2014. **48**(4): p. 2361-2367.
23. Herreros, J.M., Gill, S. S., Lefort, I., Tsolakis, A., Millington, P., Moss, E., *Enhancing the low temperature oxidation performance over a Pt and a Pt–Pd diesel oxidation catalyst.* Applied Catalysis B: Environmental, 2014. **147**: p. 835-841.
24. Mittendorfer, F., Thomazeau, C., Raybaud, P., Toulhoat, H., *Adsorption of unsaturated hydrocarbons on Pd (111) and Pt (111): A DFT study.* The Journal of Physical Chemistry B, 2003. **107**(44): p. 12287-12295.
25. Meakin, P., Donn, B., Mulholland, G. W., *Collisions between point masses and fractal aggregates.* Langmuir, 1989. **5**(2): p. 510-518.
26. Yamamoto, K., Takada, K., Kusaka, J., Kanno, Y., Nagata, M. *Influence of diesel post injection timing on HC emissions and catalytic oxidation performance*. in *Powertrain and Fluid Systems Conference and Exhibition*. 2006.
27. Chen, P., Ibrahim, U., Wang, J., *Experimental investigation of diesel and biodiesel post injections during active diesel particulate filter regenerations.* Fuel, 2014. **130**: p. 286-295.
28. Desantes, J., Bermúdez, V, Pastor, JV, Fuentes, E, *Investigation of the influence of post-injection on diesel exhaust aerosol particle size distributions.* Aerosol science and technology, 2006. **40**(1): p. 80-96.
29. O'Connor, J., and Musculus, M., *Post Injections for Soot Reduction in Diesel Engines - A Review of Current Understanding.* SAE Technical Paper, 2013: p. 01-0917.
30. Chen, S.K., *Simultaneous reduction of NOx and particulate emissions by using multiple injections in a small diesel engine*. 2000, SAE Technical Paper.
31. Sperl, A., *The Influence of Post-Injection Strategies on the Emissions of Soot and Particulate Matter in Heavy Euro V Diesel Engine.* SAE Technical Paper , 2011. **36**(0350).
32. Bobba, M., Musculus, M., Neel, W., *Effect of post injections on in-cylinder and exhaust soot for low-temperature combustion in a heavy-duty diesel engine.* SAE International Journal of Engines, 2010. **3**(1): p. 496-516.

33. Yun, H., Reitz, R. D., *An experimental investigation on the effect of post-injection strategies on combustion and emissions in the low-temperature diesel combustion regime.* Journal of Engineering for Gas Turbines and Power, 2007. **129**(1): p. 279-286.
34. Barro C., T.F., Obrecht P., Boulouchos K. *Influence of post-injection parameters on soot formation and oxidation in a common-rail-diesel engine using multi-color-pyrometry*. in *ASME 2012 internal combustion engine division fall technical conference*. 2012. American Society of Mechanical Engineers.
35. Desantes, J.M., Arrègle, J., López, J. J., García, A., *A comprehensive study of diesel combustion and emissions with post-injection*. 2007, SAE Technical Paper.
36. Poorghasemi, K., Ommi, F., Yaghmaei, H., Namaki, A., *An investigation on effect of high pressure post injection on soot and NO emissions in a DI diesel engine.* Journal of mechanical science and technology, 2012. **26**(1): p. 269-281.
37. Mohan B, Y.W.a.C.S., *Fuel injection strategies for performance improvment and emissions reduction in compression ignition engines - A review.* Renewable and Sustainable Energy Reviews, 2013. **28**: p. 664-676.
38. Valentino, G., Iannuzzi, S. E., Marchitto, L., Merola, S. S., Tornatore, C., *Optical Investigation of Postinjection Strategy Effect at the Exhaust Line of a Light-Duty Diesel Engine Supplied with Diesel/Butanol and Biodiesel Blends.* Journal of Energy Engineering, 2013. **140**(3): p. A4014010.
39. Fino, D., *Diesel emission control: Catalytic filters for particulate removal.* Science and Technology of Advanced Materials, 2007. **8**(1): p. 93-100.
40. Li, X., Guan, C., Luo, Y., Huang, Z., *Effect of multiple-injection strategies on diesel engine exhaust particle size and nanostructure.* Journal of Aerosol Science, 2015. **89**: p. 69-76.
41. Yehliu, K., Armas, O., Vander W., Randy L., Boehman, A. L., *Impact of engine operating modes and combustion phasing on the reactivity of diesel soot.* Combustion and Flame, 2013. **160**(3): p. 682-691.
42. Hiranuma, S., Takeda, Y., Kawatani, T., Doumeki, R., Nagasaki, K., Ikeda, T., *Development of DPF System for Commercial Vehicle-Basic Characteristic and Active Regenerating Performance*. 2003, SAE Technical Paper.
43. Parks, J., James, E., Huff, S. P., Kass, M. D., Storey, J. M., *Characterization of in-cylinder techniques for thermal management of diesel aftertreatment*. 2007, Oak Ridge National Laboratory (ORNL); Fuels, Engines and Emissions Research Center.
44. AVL, *Pressure Sensor for Combustion Analysis – Data Sheet GH13P [Internet]. [Cited 3 November 2015].* Available from URL: https://www.avl.com/documents/10138//885983//AT3368E_GH13P.pdf., 2011.
45. AVL, *Microifem Piezo 4th Generation – Piezo Amplifier [Internet] [Cited 3 November 2015].* Available from URL: https://www.avl.com/documents/10138//0//MicroIFEM+4P4+Piezo., 2013.
46. Lapuerta, M., Martos, F. J., Martín-González, G., *Geometrical determination of the lacunarity of agglomerates with integer fractal dimension.* Journal of colloid and interface science, 2010. **346**(1): p. 23-31.
47. Lapuerta, M.B., R.; Martos, F. J., *A method to determine the fractal dimension of diesel soot agglomerates.* J. Colloid Interface Sci., 2006. **303**: p. 149-158.
48. Westbrook, C.K., W.J. Pitz, and H.J. Curran, *Chemical kinetic modeling study of the effects of oxygenated hydrocarbons on soot emissions from diesel engines.* The journal of physical chemistry A, 2006. **110**(21): p. 6912-6922.
49. Choi, B., Jiang, Xiaolong, *Individual hydrocarbons and particulate matter emission from a turbocharged CRDI diesel engine fueled with n-butanol/diesel blends.* Fuel, 2015. **154**: p. 188-195.

50. Lee, K.O., Sekar, R., Choi, M. Y., Kang, J. S., Bae, C. S., Shin, H. D., *Morphological investigation of the microstructure, dimensions, and fractal geometry of diesel particulates.* Proceedings of the Combustion Institute, 2002. **29**(1): p. 647-653.
51. Lee, K.O., Cole, R., Sekar, R., Choi, M. Y., Z., J., Kang, J., Bae, C., *Detailed characterization of morphology and dimensions of diesel particulates via thermophoretic sampling*. 2001, SAE Technical Paper.
52. Crookes, R.J., Sivalingam, G., Nazha, M. A. A, Rajakaruna, H., *Prediction and measurement of soot particulate formation in a confined diesel fuel spray-flame at 2.1 MPa.* International journal of thermal sciences, 2003. **42**(7): p. 639-646.
53. Choi, S.C.R., Hyun G. u., Lee, K. S., Lee, C. S., *Effects of fuel injection parameters on the morphological characteristics of soot particulates and exhaust emissions from a light-duty diesel engine.* Energy & Fuels, 2010. **24**(5): p. 2875-2882.
54. Hwang, J.J., Y., Bae, C. *Particulate morphology of waste cooking oil biodiesel and diesel in a heavy duty diesel engine*. in *International Conference on Optical Particle Characterization (OPC 2014)*. 2014. International Society for Optics and Photonics.
55. Qu, L., Wang, Z., Hu, H., Li, X., Zhao, Y. , *Effects of butanol on components and morphology of particles emitted by diesel engines.* Researh of Environmental Sciences, 2015. **28**(10): p. 1518-1523.
56. Song, J., Cheenkachorn, K., Wang, J., Perez, J., Boehman, A. L., *Effect of Oxygenated Fuel on Combustion and Emissions in a Light-Duty Turbo Diesel Engine.* Energy Fuels, 2002. **16**(2): p. 294-301.
57. Chen, Z., Wu, Z., Liu, J., Lee, C., *Combustion and emission characteristics of high n-butanol/diesel ratio blend in a heavy duty diesel engine and EGR impact.* energy Conversion and Management, 2014. **78**: p. 787-795.
58. Richard K., L., J. Cole, A.. *"A reexamination of the Rapre NOx process"* . Combustion and Flame, 1990. **82**(3-4): p. 435-443.
59. Lapuerta, M., Armas, O., Rodríguez-Fernández, J., *Effect of biodiesel fuels on diesel engine emissions.* Progress in Energy and Combustion Science, 2008. **34**: p. 198-223.
60. Hajbabaei, M., Johnson, K.C., Okamoto, R., Durbin, T.D., *Evaluation of the Impacts of Biofuels on Emissions for a California Certified Diesel Fuel from Heavy-Duty Engines.* SAE Technical Paper, 2013: p. 01-1138m.
61. Diehl, F., Barbier, J., Duprez, D., Guibard, I., Mabilon, G., *Catalytic oxidation of heavy hydrocarbons over Pt/Al2O3. Influence of the structure of the molecule on its reactivity.* Applied Catalysis B: Environmental, 2010. **95**(3): p. 217-227.
62. Lapuerta, M., García-Contreras, R., Campos-Fernández, J., Dorado, M. P., *Stability, lubricity, viscosity, and cold-flow properties of alcohol– diesel blends.* Energy & fuels, 2010. **24**(8): p. 4497-4502.